Provisional chapter

Developmental Plasticity: fMRI Investigations into Human Visual Cortex

Alyssa A. Brewer and Brian Barton

Additional information is available at the end of the chapter

1. Introduction

The ultimate goal of many fields of neuroscience research is to harness the ability for the human brain to reorganize, as an understanding of how to induce plasticity in cortex could foster the development of treatments of such devastating conditions as paralysis, neurodegenerative disease and stroke. The specifics of the timing and types of reorganization possible in cortical sensorimotor maps have generated tremendous interest, both in the adult and juvenile brain. While it is clear that cortical representations in human are able to undergo significant reorganization during development (an early critical period of life) (e.g., [1-4]), the extent of reorganization possible in the developing human brain is still not fully known. In addition, there are likely differences in the timing and degree of reorganization possible across the different sensory modalities [5-11]. This chapter will focus on examples of plasticity in the visual cortex of the developing human arising from congenital disorders, with specific attention to the use of functional magnetic resonance imaging (fMRI) in in vivo measurements of these cortical changes.

1.1. The definition of plasticity

The phenomenon we refer to as 'structural plasticity' will be defined as the long-term reorganization of human visual cortex due to a structural change such as the growth of new axons [5] (Table 1). This type of reorganization is generally expected to be permanent and to take weeks or months to accomplish [12]. 'Structural plasticity' is to be differentiated from 'adaptation', which we use here to refer to rapid changes in visual processing arising from the normal organization of the visual system and not a result of long-term reorganization (see [5] for a detailed discussion of terms). Phenomena of adaptation are expected to be immediate and completely reversible. Furthermore, these two terms are to be separated from

'functional plasticity', which we will use to describe longer-term reorganization of human visual cortex, primarily due to re-weighting or unmasking of extant neural connections rather than to more extensive structural changes like the growth of new axons. Functional plasticity is expected to take days to weeks to accomplish, and it is still unclear how permanent it can be. At one point or another, each of these terms has been described using the term 'plasticity', and we would like to put an end to this non-specificity, as it leads to misunderstandings regarding each phenomenon.

1.2. Overview of developmental plasticity in the visual cortex of animal models

Many aspects of the development of the visual system have been extensively studied in animal models such as monkey and cat. The mammalian visual system develops in a balance between intrinsic, genetically-guided factors and activity-based experience [13-17]. The ability of the brain to wire and rewire itself based on visual input is known as experience-dependent plasticity (a form of structural plasticity) and plays a key role in determining the final organization of adult visual cortex [1, 12, 15, 18]. The following descriptions of visual cortex development in animal models can serve here as examples of what processes may underlie the visual cortex reorganization described in this chapter for the developing human.

In human and monkey, visual information travels from the retina through the lateral geniculate nucleus (LGN) of the thalamus to primary visual cortex (area V1) in the posterior occipital lobe [19]. In the adult primate, the inputs from each eye are organized into separate groups within V1 called ocular dominance (OD) columns [20]. Emerging from a literature which viewed the immature brain as a haphazardly wired structure that undergoes large-scale remodeling at birth to form OD columns, Hubel and Wiesel were surprised to find that the OD columns within primary visual cortex are actually organized at birth in an adult-like pattern [21-23]. Several subsequent studies investigated whether visual experience (e.g., light stimulation) is necessary for development of the mature pattern of OD columns seen in the infant brain [22-25]. Horton and Hocking [20] finally resolved the issue with heroic measurements of completely dark-reared infant macaque monkeys; the OD columns in these monkeys with no visual experience are organized like those measured in the adult macaque. Other features of cortical functional architecture, such as orientation tuning and orientation columns, are also present before any visual experience [15].

Further experiments investigating how this initial functional architecture is formed have unveiled activity-dependent processes that operate even before the retinal photoreceptors are functional and play a key role in determining the OD organization [16]. In utero, spontaneous coordinated waves of retinal ganglion cell action potentials are required for the development of normal OD and orientation columns [13, 15, 26, 27]. Thus, patterned retinal inputs to the cortex modify initially imprecise connections to produce an organized visual topography prior to the visual experience.

In turn, visual experience during an early critical period of life can profoundly alter the cortical visual topography formed by the in utero retinal activity [14, 18]. For example, if one eye is deprived of vision for several weeks in infancy, then most of the mature visual cortical neurons are responsive only to stimuli presented to the eye that remained open; the cortical

territory normally devoted to the closed eye is greatly diminished [18, 21]. This reorganization causes a loss of perception in the eye that was closed, as seen in cases of congenital cataracts leading to amblyopia and life-long blindness [28-31].

Measurement	*Structural Plasticity*	*Functional Plasticity*	*Adaptation*
Temporal scale of cause	Longer than inciting factor	Longer than inciting factor	Short (~tracking input statistics)
Temporal scale of effect	Weeks to months	Days to weeks	Short (~tracking input statistics)
Anatomical connectivity	New connections	Likely re-weighted existing connections	Unlikely to change
Receptive field: Location	May change	May change	May change
Receptive field: Size	May change	May change	May change
Receptive field: Gain	May change	May change	May change
Reversibility	Not typical	Yes, in days to weeks	Yes, within a short time

Table 1 Characteristics of Plasticity and Adaptation. This table delineates core characteristics of three types of 'plasticity': structural plasticity, functional plasticity, and adaptation. Differentiating between each of the three can be difficult, because many measurements do not distinguish one type from another. In addition, there are not always sharp distinctions between the three phenomena. Confusion and controversy have often arisen from the non-specific use of the term 'plasticity' to describe these different cortical changes. This table is adapted and expanded from Box 1 in [5], a prominent review of plasticity and stability of the visual system.

1.3. Using the topography of visual cortex to track changes in human development

These examples of visual cortical development were studied in animal models using such invasive techniques as electrophysiology and histology. How can we study cortical changes in the living, developing human? One technique that is proving very effective is to measure visual field maps (VFMs) in human visual cortex with functional magnetic resonance imaging (fMRI) to study cortical reorganization in response to abnormal visual input [5].

Human visual cortex is organized into distinct VFMs whose locations and properties provide important information about visual computations [32-35]. In each retinotopically-organized VFM, neurons whose visual receptive fields lie next to one another in visual space are located next to one another in cortex, forming one complete representation of contralateral visual space. By taking advantage of the knowledge of the retinotopic organization of visual input, multiple cortical VFMs can be measured using fMRI with respect to the two orthogonal dimensions needed to identify a unique location in visual space: eccentricity and polar angle (Figs. 3A, 4A, 5A). Each VFM subserves a specific computation or set of computations; locating these VFMs allows for the systematic exploration of these computations across visual cortex [33, 36].

Understanding the organization of these maps provides a baseline for studying reorganization following abnormal development or cortical damage. This chapter will review a series

of studies of human developmental visual plasticity that capitalize on our ability to measure these VFMs with a high level of detail in individual subjects. We examine genetic, retinal, and cortical alterations that lead to reorganization of the cortical VFM organization. These examples of cortical developmental plasticity give us insight into the flexibility and constraints present in the human visual system.

2. Methods

2.1. General fMRI methods

Measurements of VFMs in human require very precise fMRI measurements and highly detailed, individual subject analysis [32, 34]. Before delving into the details of the two main types of fMRI experimental techniques used to measure VFMs, it is vital to remember that all fMRI techniques are empowered and limited by four common factors: the properties of fMRI in general, subject biology, experimental stimuli, and statistical analysis. Regardless of the cleverness of the experimental design, basic errors in any of these categories run the risk of rendering an entire study irrelevant due to inaccurate or misinterpreted results [37]. We will briefly review these factors with respect to their importance to visual field mapping.

2.1.1. Properties of fMRI

Let's begin with the basics of fMRI. When neurons are active consequent to task-induced or spontaneous neural metabolic modulations, the ratio of diamagnetic, oxygenated hemoglobin to paramagnetic, deoxygenated hemoglobin in nearby blood increases after a few seconds with a characteristic profile, called the hemodynamic response function (HRF; for reviews and more details, see [38-41]). fMRI is a technique that takes advantage of such blood oxygen-level dependent (BOLD) activity in the brain by applying a strong magnetic field and encoding positions in space through slight differences in magnetic field strength and phase [40, 42]. This allows for a very specific spatial readout of brain activity (on the order of 1 mm^3, often in the 1-4 mm^3 range), but the hemodynamic response is on the order of seconds, which limits the ability of fMRI to distinguish fine temporal differences [43].

Scanners suitable for human research commonly have a magnetic field strength of 1, 1.5, 3, or 4 Tesla (T), though access to 7T scanners is becoming more common. The field strength affects many aspects of the scanning parameters that can be chosen, but there is a basic trade-off between spatial resolution and signal-to-noise ratio (SNR), although different field strengths may also suffer from differing distortions or artifacts [44-46]. Lower field strength gives researchers a lower SNR, which forces researchers to use larger voxels. A larger voxel size increases SNR, because signal can be averaged across a greater number of active neurons within a voxel. However, large voxels also reduce spatial detail, which is important for advanced fMRI techniques such as those used for visual field mapping [34, 38, 47]. A key element for making careful, accurate measurements of plasticity in human cortex is to be able to acquire both high spatial resolution images and high SNR. Naturally, there are many

other details to consider in the scanning parameters, but these are outside the scope of the chapter.

2.1.2. Subject cortical biology

The basic properties of fMRI scanners quickly become more complicated when biological factors are taken into account [39, 48, 49]. Air cavities, like the frontal sinuses or the ear canals, can create 'blow-out' artifacts in the images of the nearby portions of brain by locally distorting the magnetic fields [50]. Although less relevant for most measurements of visual cortex, it is a factor that should not be ignored. For example, if one were to compare visual activity in primary visual cortex to visual activity near these distorted regions, one may make incorrect inferences about activity level differences that have little to do with the experiment but instead are driven by these distortions [34, 38, 39, 48, 49, 51].

Another consideration is the arterial and venial physiology of individual subjects. Large draining veins may create distortions in the fMRI signal arising from neighboring cortex [52]. These distortions are unpredictable due both to the sensitivity of these distortions to the relative magnetic gradients and to the high variability of the venous system across individuals. For example, Winawer et al. [53] demonstrated the role for a 'venous eclipse' in the difficulties in measuring of the contiguous hV4 hemifield representation on the human ventral occipital cortex. These difficulties led to several years of confusion and controversy regarding the VFM organization in this region [33, 54-59].

It is also important to take the cortical anatomy of the individual subject into account. Although it is becoming more common practice in some fields to segment out white from gray matter and consider only activity occurring in gray matter, this is still not the standard approach [39]. As far as is currently known, the primary neural computations take place in gray matter; therefore, one should only consider activity in biologically relevant tissue, particularly when comparing regions of interest that could, without considering only gray matter, include different amounts of white matter as frequently occurs in typical slice-based analysis [60]. It should also be noted that not all white-gray matter segmentation is created equal—there are several algorithms used to parcel them out, but all require hand-editing for appropriate accuracy, which can be time intensive [32, 61-63].

2.1.3. Experimental stimuli

For any field of visual neuroimaging research, one must be incredibly careful in the choice of experimental stimuli, especially when contrasting activity between two or more types of stimuli. First, one must take into account the retinotopic nature of large portions of visual cortex [32-34, 64] and present stimuli in retinotopically consistent locations (unless activity is being measured for different locations of the visual field). Next, stimuli must be chosen that are equivalent on every aspect except those of interest. Unaccounted-for features can explain the results of interest when low-level features of stimuli are ignored in favor of interpreting data in terms of perceptual categories (e.g., [65, 66]).

2.1.4. Statistical analysis

In the unending search for statistical significance, researchers often use some variety of spatial averaging across subjects in order to increase their statistical power. There are two primary approaches to spatial brain averaging: morph individual subject brains onto a template brain or average locally based on local anatomical landmarks. From a behavioral experimental perspective, this may seem as reasonable as averaging together d-prime scores for individual subjects, but that is far from the case. One must take into account the inter-subject biological variability, not just in the location of veins, but of every aspect of the brain. Individual, neurologically normal subjects may have extra, missing, differently sized or differently folded gyri and sulci [67, 68]. The cortical surface of primary visual cortex, V1, can vary by a factor of ~2.5 among normal subjects, which not only affects the measurement of V1, but of all neighboring regions as a result of the displacement with respect to the underlying anatomy [69]. Although likely less problematic for vision, handedness has also been implicated in differences between hemispheric organization [70, 71]. Also, overall brain size can vary not only by gender, but by skull and body size. Additionally, skull shape can vary, shifting locations of individual brain regions due to the brain displacement relative to other subjects [72]. Obviously this is not an exhaustive list of normal variation, and it doesn't even take into account the wide variety of possibilities for damage in people who self-report being neurologically normal—or the differences between patients with similar neurological conditions within a particular study of visual plasticity.

Despite these issues, the vast majority of researchers use spatial averaging. The only truly viable solution is functional averaging, which is where regions of interest (ROIs) are defined based on functional data, then data from corresponding ROIs across subjects are averaged together. For example, if one wanted to study color activity in hV4, one would first use a visual field mapping technique to map hV4 in each subject (see Travelling Wave Retinotopy and Population Receptive Field Modeling sections below), then average together color activity for each subject from their individually defined hV4 maps [32, 54]. In this way, each subject's unique brain is taken into account rather than being distorted to approximate a template, and the relevant information is still averaged across subjects.

Finally, let us consider another common practice: spatial smoothing. This is when researchers average together activity in nearby voxels, often using a several-millimeter Gaussian kernel. What this allows researchers to do is to smooth the data for each voxel, reducing overall signal variability. However, such smoothing eliminates detailed information in the process. While this may be acceptable when one's technique cannot utilize detailed spatial information, it is disastrous when applied to detailed information such as that contained in VFMs [33, 58].

2.2. Travelling Wave Retinotopy

Travelling Wave Retinotopy (TWR) was developed to measure retinotopically organized visual cortex. To do so, TWR takes advantage of knowledge gleaned from electrophysiological measurements of visual cortex in animal models about the structure and stimulus preferences of VFMs. Because many computations are required to create our visual experience,

our brains have many specialized VFMs which perform one or more of those computations across the entire visual scene (e.g., motion perception happens throughout our visual field, not just in the upper left quadrant).

Taking advantage of this knowledge, TWR uses two types of stimuli to measure the two orthogonal dimensions of visual space: eccentricity (i.e., center to periphery) and polar angle (i.e., around the clock) [32, 34, 73-76] (Figs. 3A, 4A). These stimuli tile across as much of the visual field as possible given field of view limitations with the MR scanner. The first stimulus is designed to elicit each voxel's preferred eccentricity by presenting a high-contrast flickering stimulus shaped like a ring, expanding in discrete even steps from the center of vision (fixation) to the periphery. The second is designed to elicit each voxel's preferred polar angle by presenting a high-contrast flickering stimulus shaped like a wedge that extends from the fovea to periphery, which rotates in discrete even steps around the fixation point. A checkerboard pattern commonly comprises the high contrast stimulus, as this pattern maximally stimulates V1; however, any pattern of interest can theoretically be used [77]. In each scan, only one type of stimulus is presented (rings or wedges), and all of visual space is cycled through several times with each stimulus (Fig. 1). Typically, several scans are then averaged together for each stimulus type. The type of activity driven by these stimuli physically appears to be a wave that travels from one end of the VFM to the other along iso-angle or iso–eccentricity lines, giving TWR its name.

The design of TWR presents all eccentricities or polar angles at a given frequency per scan (typically 6-8), which allows the use of Fourier analysis. First, TWR only considers activity that is at the signal frequency (typically 6-8 cycles/scan), excluding low-frequency physiological noise, among other things. A coherence analysis is then performed, where the strength at the signal frequency is divided by the strength at the other frequencies, and only voxels with coherence above a threshold are further evaluated (typically 0.15 to 0.30 coherence) [32, 34]. Finally, a phase is assigned to each voxel, which corresponds to a particular eccentricity or polar angle preference (Fig. 1).

Between these measurements of eccentricity and polar angle, TWR provides an estimate of the preferred RF center of the population of neurons with visual RFs in each voxel (Fig. 2). This technique is excellent at driving activity in early retinotopic areas (e.g., V1, V2, V3, hV4), in which neural RFs are relatively small [73, 74, 78, 79]. However, VFMs with larger neural RFs (e.g., regions in lateral-occipital cortex) are more difficult to measure, because the voxels respond to large swaths of the visual field [33, 78-80]. Even with large receptive fields, regions can still be retinotopically organized with retinotopically dispersed, preferred receptive field centers [32]. This large response field means that several TWR stimulus positions can similarly activate such a region. Because TWR analysis relies on measuring cortical responses in sync with the stimulus movement, regions that activate to a specific set of multiple stimulus positions may appear to have lower or no retinotopic responses, even with retinotopically dispersed RF centers.

Additionally, VFMs that have a larger degree of RF scatter within each voxel are more difficult to measure for the same reasons as large neural RFs. As a result of the power of TWR, it has become the standard workhorse for localizing and measuring the spatial details of

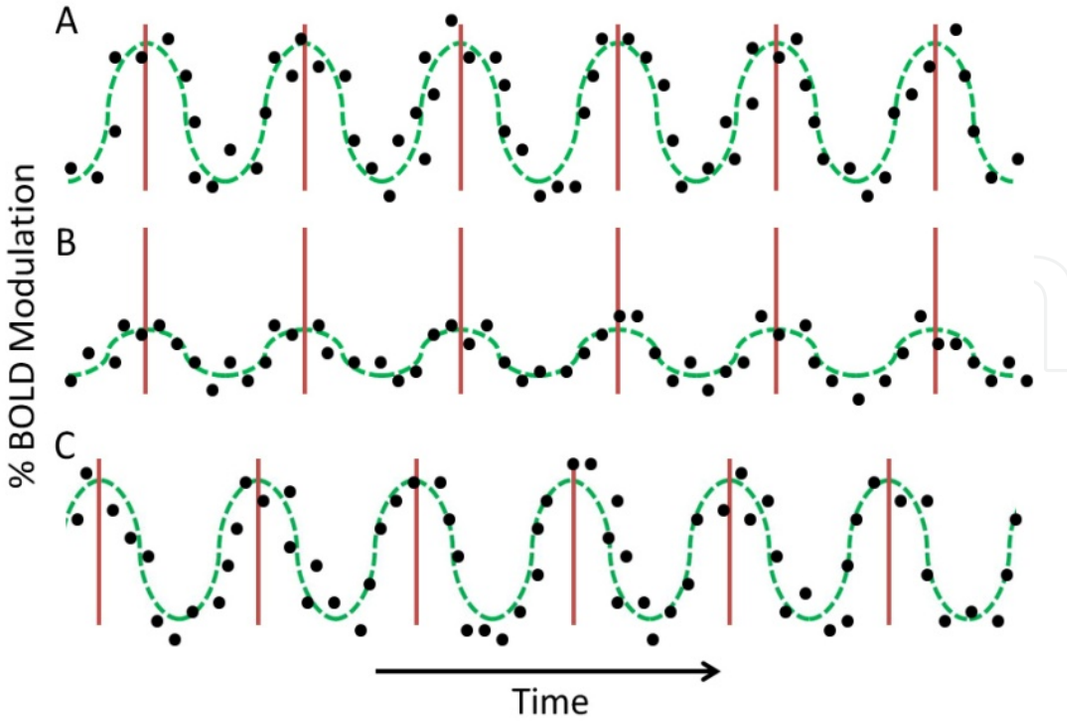

Figure 1. Visual Field Mapping Time Series Analysis. Each row represents the activity and analysis of a time series of a single 6-cycle scan of one type of experimental stimuli (expanding rings or rotating wedges) for a single voxel. Black dots indicate simulated raw data points of % BOLD modulation. The red lines indicate the peak activations per cycle for an imaginary set of voxels, which are the measurements used by the TWR analysis. The green dotted line represents a sinusoidal fit of the simulated data points, which are the measurements used by pRF modeling. Rows (A) and (B) represent time series of voxels with identical peak responses, indicating identical stimulus selectivity. However, (B) has much lower %BOLD modulation than (A), which could be due to two common factors: differences in local vasculature or broader receptive field tuning for (B) than (A). Rows (A) and (C) represent time series of voxels with identical %BOLD modulation, but different peak responses, which indicate different stimulus selectivity (i.e., different 'phases' of response). For example, (A) might represent a voxel with a preferred eccentricity tuning of 5° eccentric to fixation, whereas (C) might have a preferred tuning of only 2° eccentric to fixation.

VFMs. Relative to other neuroimaging methods like general condition contrast (GCC) approaches, TWR provides an unprecedented amount of detail [32, 33, 77]. For example, while the GCC may reveal the location of a large cluster of voxels that has been termed the human motion complex, hMT+, TWR reveals several distinct, highly organized VFMs within that large voxel cluster [64, 81].

2.3. Population receptive field modeling

The most recently developed technique of those covered in this chapter is population receptive field (pRF) modeling [78]. Once it had become clear that there were serious limits to the ability of TWR to deal with VFMs with large RFs, researchers at Stanford University decided that the best solution was to use a model of the pRFs of each voxel in VFMs [78]. This approach arose in part from previous work in several studies [30, 57, 79, 82, 83], which measured receptive fields in human and macaque visual cortex. The logic of pRF

modeling is that, because VFMs are retinotopically organized, the population of RFs in each voxel of a VFM is expected to have similar preferred centers and sizes, allowing their combined pRFs to be estimated as a single, two-dimensional Gaussian RF (Fig. 2). Despite the fact that there is some variability in the neural RFs of each voxel in terms of their preferred center and size, termed RF scatter, the pRF provides a good, if somewhat slightly larger, estimate of the individual neural RFs in the voxel [78, 81, 84].

The advantages of the method are generally stated in comparison to the field standard for measuring VFMs, TWR. Not only does pRF modeling allow for the measurement of the preferred centers of the pRF of a voxel like TWR, but it also measures the spatial spread of the pRF, allows for the use of any stimulus that systematically tiles visual space, and takes less scan time to do, as it can use a single stimulus like a moving bar to measure both dimensions of visual space.

To accomplish this, the pRF model first creates a database of all possible pRF sizes and centers given the field of view of the stimulus used. Then, the model creates an expected HRF profile for each of the pRF possibilities based on an assumed or individually measured HRF. Finally, the model uses a least-squares fitting method to iteratively test each of the pRF possibilities for each voxel independently against the actual data collected [78]. Whichever pRF best fits the data is then assigned as the pRF for that voxel. Voxels are discarded if they do not have above a threshold of variance explained by the model. Although it is technically possible to use any stimulus that traverses the entire field of view, typically the stimuli take one of two forms. First is a slightly modified version of the TWR stimuli, in which neutral gray blank periods are inserted at an off-frequency from the stimulus frequency (e.g., 4 instead of 6-8 cycles/scan, so they are separable in the Fourier analysis). The second and increasingly common stimulus is a high-contrast flickering checkerboard moving bar stimulus that steps across the field of view in the 8 cardinal directions, again with several interspersed neutral gray blank periods. In theory, one could also tile visual space using any stimulus of interest, if the aforementioned stimuli do not drive the cortical region well. Since they were designed to drive activity in early visual cortex, it is possible other stimuli may perform better in higher-order VFMs [85, 86].

Because pRF modeling has proven so successful, we expect that it will eventually replace TWR as the standard method for measuring VFMs. Moreover, pRF modeling has an excellent future in the measurement of the details of pRFs, which is particularly important for the measurement of visual plasticity in humans. So far, the technique has primarily used a two-dimensional Gaussian profile for the pRF estimates, but researchers are working on the use of center-surround Gaussian pRFs, multiple location pRFs, and non-classical pRF shapes, which may allow for better pRF estimation as time continues [87]. For its purpose, the limitations of the pRF modeling method are essentially the measurement limitations of the scanner and stimuli used. In the future, it is likely that pRF modeling will be very successful when used in isolation, but also excellent to use in conjunction with other techniques.

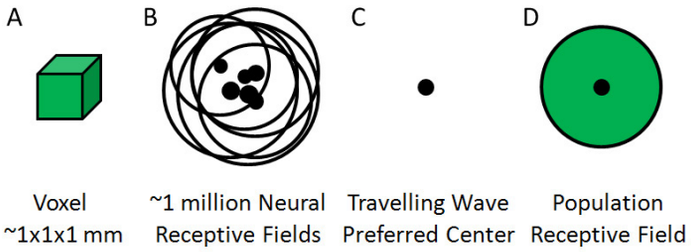

Figure 2. Measurements of an Individual Voxel. (A) A typical voxel recorded from a 3T MRI scanner is on the order of 1 mm^3, though often slightly larger (2-3 mm^3). (B) Within each typical voxel, there are on the order of ~1 million neurons, depending on the size of the voxel. For voxels in retinotopic visual cortex, the neurons each have similarly located spatial receptive fields (black outlines) with preferred centers (black dots). (C) TWR takes advantage of the fact that nearby neurons in retinotopic cortex have similar preferred centers in order to estimate a population preferred center for the population of neurons in a given voxel. (D) pRF modeling takes advantage of the fact that nearby neurons in retinotopic cortex have similar receptive fields in order to estimate not only a preferred center, but also a pRF for the population of neurons in a given voxel.

3. Developmental plasticity following congenital lesions

Cortical reorganization is generally accepted by neuroscientists as a fact of life during development. Along the way to adulthood, neural structures grow, sprout, connect, and are pruned in a series of complex cascades and critical periods. In short, cortical reorganization not only happens during development, it's rampant. Perhaps that is why there is less controversy surrounding claims of cortical plasticity as a result of congenital abnormalities. As a rule, the developing brain is more plastic than the adult brain, but in both cases, the brain is striking a balance between plasticity and stability [5].

For the visual system, the balance is decidedly skewed towards stability, except in the earlier stages of development [88]. Stability is very useful for the visual system in the adult, because there are very few circumstances under which changes in properties of neurons in visual cortex such as their spatial representations is beneficial after development [6]. In fact, in most circumstances, it would be costly and destructive to change visual circuitry in the brain. In effect, each portion of visual space has its own processing pipeline through the visual hierarchy, which is possible only if independent processing channels for each portion of space are maintained. If the visual system were highly plastic, portions of the visual field would necessarily be cross-wiring these processing pipelines, disrupting the processing hierarchy in chaotic fashion wherever a crossing occurred. Contrast this with the memory systems of the brain, which could not possibly function without a high degree of plasticity to encode memories and associate them with one another (e.g., [89]). Of course, memory systems are not entirely plastic, as memories must also be maintained, but the balance point between plasticity and stability is quite different from that of the visual system.

In the congenital orders described here, developmental alterations of the organization of visual input to cortex are expected to drive the reorganization of visual representations in visual cortex. This reorganization of cortical visual representations might occur in one or more of

the following ways (e.g., [5, 90]). First, major changes in the visual input to cortex may lead to a total disruption of retinotopic organization in visual cortex. Second, major retinal changes may lead to a reorganization of a section of cortical visual representation in response to a loss of retinal activity for a portion of visual space. Third, altered visual pathways could lead to a restriction of the field of view as cortical maps reach a limit on how much of the contra- and ipsilateral hemifields could be represented in each hemisphere. Fourth, changes in the crossing of the visual pathways could lead to larger-than-normal, contiguous representations of visual space representing more than the normal contralateral hemifield. Finally, such changes in visual pathways could produce overlapped visual field representations, in which an abnormal representation of the ipsilateral visual field is superimposed on the representation of the normal contralateral visual field. In a single congenital disorder affecting the visual system, one or even several such changes in cortical visual representations could theoretically be present. Measurements of what types of reorganization actually appear in these disorders highlight the capabilities for adaptation to altered visual inputs in human visual cortex.

The abnormal drivers of developmental plasticity in the visual system can be grouped into three major categories. The first are retinal lesions, in which visual information about a location is never present in the visual system because of a functional failure in retinal circuitry. The second are altered visual pathways, in which visual information is misrouted from the retina to its intended thalamic or cortical targets. Finally, we have cortical lesions, in which visual information enters the visual system, but undergoes abnormal processing due to a disruption in the cortical processing hierarchy. The following sections will describe examples from each category that were studied in human subjects using fMRI.

3.1. Congenital retinal lesions can produce changes in cortical visuospatial representations

3.1.1. Rod monochromatism

Two primary classes of photoreceptors tile the human retina: cones, which are maximally responsive under normal lighting (photopic) conditions, and rods, which are maximally responsive under very low lighting (scotopic) conditions [91]. The cones are highly concentrated in the fovea of each retina, whereas the concentration of rods drops dramatically and becomes zero within a radius of ~0.6-0.8° of visual angle about the eyes' fixation point [91-93]. While the rod-free fovea occupies <1% of the retina, the cortical representation of this retinal region occupies roughly 20% of primary visual cortex [94].

Under scotopic conditions, normal subjects perceive a scotoma ~2-4° of visual angle in diameter at the center of their vision [93, 95-97]. This rod scotoma, like the blind spot, is functionally equivalent to a retinal lesion—light falls on a location in the retina but is not processed due to a lack of active photoreceptors (Fig. 3AB). Recent research indicates that the rod scotoma in normal adults does not fill-in lines or patterns or color, as rods alone do not give rise to color [97], but does fill-in diffusely lit surfaces [98]. The differences in filling-in properties of the rod scotoma from those of the blind spot likely are due to the differences in their cortical receptive field sizes (small vs. large), their ocularity (binocular vs. monocular),

their retinal locations (central vs. peripheral), and their physical exposures (infrequent vs. constant). Regardless, the cortical representation of the rod scotoma provides a natural testing ground for hypotheses regarding visual plasticity in response to retinal lesions.

Because we have invented many clever ways of maintaining photopic conditions outside of natural sunlight, modern humans are exposed to scotopic vision, and the rod scotoma, rather infrequently. Under normal conditions, occasional exposure to the rod scotoma, with cones inactive and rods active, throughout development and adulthood is not enough to induce cortical plasticity. For example, in adulthood, cortical representations of the fovea do not shift after prolonged exposure of one week to purely scotopic conditions. This was tested by Baseler et al. [95], who used TWR under photopic and scotopic conditions in normal subjects to map out the portions of V1 that represent the rod scotoma. They found no evidence for reorganization in these normal subjects either in the short term or after one week of adaptation. In fact, the region representing the rod-free fovea under photopic conditions was simply inactive under scotopic conditions, as expected from a lack of signal from the retina (Fig. 3AB).

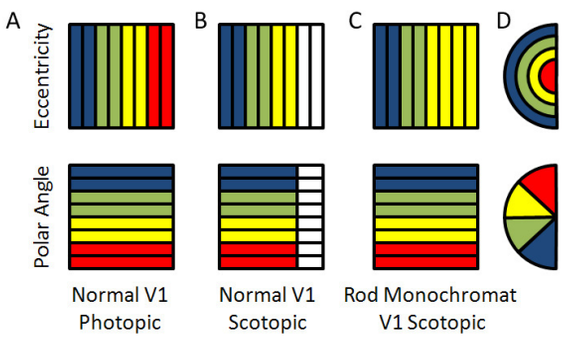

Figure 3. Visual Field Maps in Normal and Rod Monochromat Subjects. (A) Top: Eccentricity gradient for a VFM in a subject with normal vision viewing the stimulus under photopic (daylight) light conditions. Note the gradient running from the center to more peripheral eccentricities runs from right to left. This gradient would be orthogonal to the polar angle gradient in the bottom panel, such that each iso-eccentricity line has a representation of the full range of polar angles. The combination of the orthogonal gradients in top and bottom panels forms one complete representation of a hemifield of visual space. This forms one half of a complete VFM, with the corresponding half being located in the opposite hemisphere of the brain. Because the hemifield represented in this cartoon is the left (see legend in (D)), this map would be located in the right hemisphere. The colors denote positions in visual space represented in each cortical location. Note that the red colors depicting the center of space are represented in this cartoon VFM for a normal subject under photopic conditions. (B) Top: Eccentricity gradient for a VFM in a subject with normal vision viewing the stimulus under scotopic (starlight) light conditions. Bottom: Polar angle gradient of the same VFM, in the same subject under scotopic conditions. Note that the red colors depicting the center of space are not represented in the eccentricity gradient, nor are the corresponding locations of the polar angle gradient. The reason is that, under scotopic conditions, a normal subject has a "rod scotoma" at the center of their gaze where there are few-to-no rod photoreceptors; thus the portions of the VFM representing the center of gaze are not activated. (C) Top: Eccentricity gradient for a VFM in a rod monochromat under scotopic conditions. Bottom: Polar angle gradient for a VFM in a rod monochromat under scotopic conditions. Note that the red colors in the top panel of (A) have been replaced with yellow colors of (C), and that the corresponding locations in the lower panel of (C) are active, unlike the same location in the bottom panel of (B). The reason for this is that the rod monochromat's VFM has reorganized, such that regions of the VFM that would have represented the rod-free fovea now represents regions just outside. (D) Top: Visual space legend for eccentricity. Each color represents an iso-eccentricity line in the left visual hemifield. Bottom: Visual space legend for polar angle. Each color represents an iso-polar angle line in the left visual hemifield.

What if, instead, you were exposed to the rod scotoma for every moment your eyes were open since birth? Would the cortical region that would normally represent the rod-free fovea remain inactive, or would this region of cortex reorganize to represent a still-active, rod-driven region of the retina? These questions can be investigated in a particular group of subjects called rod monochromats, who lack retinal cone function. This loss of cone function is due to a specific genetic mutation in the cone cells that disrupts the phototransduction cascade in all three types of cone photoreceptors [99, 100]; the cones are present in the retina in normal locations and density, but do not respond to stimulation by light [101]. As a result, rod monochromats depend upon only their rod photoreceptors to see and, as such, have been constantly exposed to the rod scotoma throughout development and into adulthood.

Baseler et al. [95] also used TWR under photopic and scotopic conditions to map out the region of V1 devoted to processing the rod scotoma in rod monochromats. In contrast to the results in normal subjects, their measurements showed that the rod monochromats had significant activity under both photopic and scotopic conditions in the region of V1 that would be expected to represent the rod-free scotoma (Fig. 3C). In addition, this cortical activity now represented parafoveal input; this cortical region had reorganized in rod monochromats to receive input from the region of retina surrounding the rod-free fovea. This result indicates that constant exposure to the rod scotoma throughout development leads to cortical reorganization, while infrequent exposure does not.

3.2. Genetic mutations that alter the optic nerves lead to significant alterations in cortical visual field map organization

3.2.1. Albinism

The most obvious abnormality associated with albinism is the lack of normal pigmentation of the skin, hair, and eyes due to a defect in melanin production [102]. A lesser-known abnormality is albinism's disruptive effect on the development of the visual pathways, in which abnormal projections from each temporal retina carry additional ipsilateral information to each V1 [103-105]. Typically, each cortical hemisphere primarily represents the one contralateral hemifield of visual space (Fig. 4A), but with the abnormal projections in albinism each hemisphere represents a greater span of the visual field from the contralateral eye [106] (Fig. 4B). The question, then, is what happens with that information? Is the abnormal ipsilateral information simply suppressed, such that a normal contralateral hemifield representation is maintained in visual cortex, but with, perhaps, abnormal visual perception from the missing ipsilateral coverage? Or, do the projections lead to integrated representations of the ipsilateral information from the temporal retina? If the latter, how are these ipsilateral visual representations integrated into the normal contralateral ones?

Previous electrophysiological research in non-primate albino mammals has suggested that the genetic mutations that underlie albinism can drive different degrees of topographical reorganization in cortex (for review, see [105]). In one organizational pattern measured primarily in Siamese cats and albino ferrets that is called the 'Boston' pattern, the abnormal pathways are reorganized within the projections from the thalamus to cortex, which leads to

a contiguous representation of the abnormal and normal representations of visual space within visual cortex [105, 107-109]. In a second pattern called 'Midwestern' that is also seen in these mammals, the abnormal visual projections continue from the thalamus into visual cortex without reordering into a contiguous map with concurrent cortical suppression of the abnormally projecting pathways [105, 110]. The visual perceptual dysfunction in these patterns appears in some measurements to include a lack of behavioral sensitivity to the temporal retina [107, 111]. Both patterns have actually been measured within the primary visual cortex of the same animal [112].

The third and rarest pattern, called the 'true albino' pattern, has been measured in one non-human primate as well as a few albino mammals. These electrophysiological measurements suggested that this pattern lacks the reordering of inputs into cortex, forming a superimposed set of inputs from nasal and temporal retinae, but unlike the cortical suppression suggested in the 'Midwestern' pattern, these superimposed inputs are functional [113].

The use of electrophysiology in these studies makes the analysis of the broad organization of visual space across a cortical region difficult. The differing organizational patterns within discrete sections of primary visual cortex in individual albino animals highlights the importance of being able to examine larger regions of the cortical topography than provided by electrophysiological measurements. Functional MRI, however, provides excellent spatial resolution for visual field measurements across a broad field of view, the type of measurement necessary to fully examine the cortical pattern of the representations of visual space across larger swaths of cortex than possible with electrophysiology. In addition, fMRI more easily allows for analysis across a greater number of subjects, important to fully understand the extent of variations possible across individual subjects. Finally, the non-invasive nature of fMRI permits investigation into the effects of albinism on human cortical development.

A recent fMRI study by Hoffman et al. [114] used TWR to map out the cortical representations of visual space in VFMs V1, V2, and V3 in human subjects with ocular or oculocutaneous albinism. They found that the ipsilateral information from the temporal retina is abnormally represented in cortex and forms a mirror-image map in V1 that is superimposed on top of the normal contralateral representation from the nasal retinal projections, following the 'true albino pattern' [113] (Fig. 4; also see [104, 106]). This causes each voxel in V1 to represent two visual field locations that are mirrored around the vertical meridian. A similar pattern of integration was measured in VFMs V2 and V3. Together with the previous study in non-human primates, these results suggest that the developmental mechanisms that subserve the reorganization of thalamocortical projections in non-primate albino mammals are not active in albino primates, leading to a more exclusive 'true albino' pattern of topographical integration in primates.

A few further studies have explored how this abnormal integration of the retinal projections into early visual cortex representations relates to the deficits in visual perception described in albinism. In contrast to the results seen in several animal studies [107, 111], Hoffman et al. [115, 116] and Klemen et al. [117] found no visual field deficits related to the abnormal visual projections and cortical representations. Thus, human albinism presents an excellent ex-

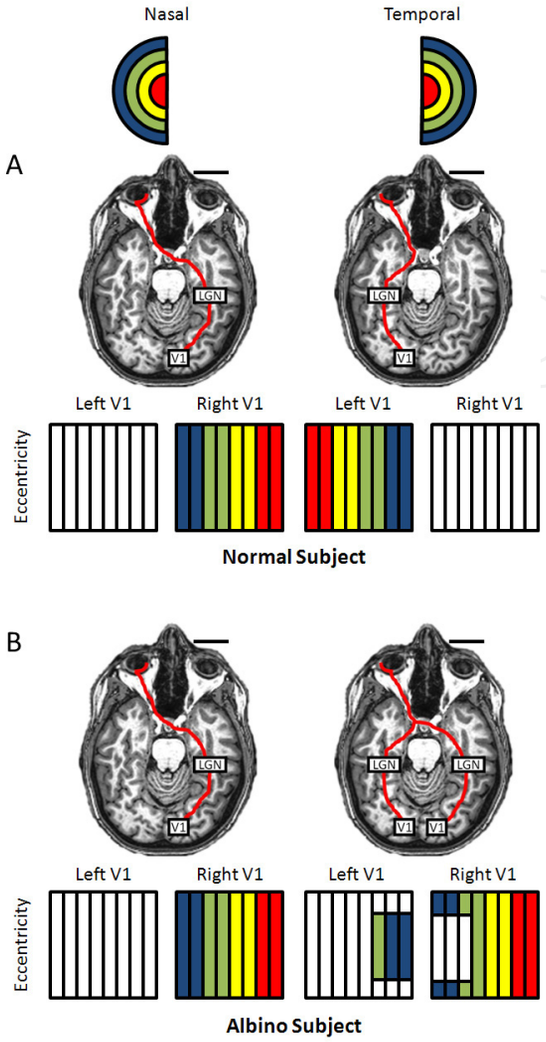

Figure 4. Visual Field Projections in Normal and Albino Subjects. In all panels, the right eye is covered with an eye patch, and only information from the left eye reaches visual cortex. The left column concerns cases where the left side of visual space, which corresponds to the nasal retina of the left eye, is stimulated. The right column concerns cases where the right side of visual space, which corresponds to the temporal retina of the left eye, is stimulated. Top row: Eccentricity visual space legend. Each color represents an iso-eccentricity line in the visual hemifield. (A) Normal subject. Top row: Information flow from the retina to visual cortex. Note that the left side of visual space (nasal retina, left column) is passed to the right hemisphere, whereas the right side of visual space (temporal retina, right column) is passed to the left hemisphere. Bottom row: Eccentricity gradient response for left and right V1. Colors represent locations in visual space denoted by the legend at the top of the figure. Note that the left side of visual space (nasal retina, left column) is represented in right V1, whereas the right side of visual space (temporal retina, right column) is represented in left V1. (B) Albino subject. Top row: Information flow from the retina to visual cortex. Note that the left side of visual space (nasal retina, left column) is passed to the right hemisphere, as in the normal subject in (A). However, unlike the normal subject in (A), the majority of the right side of visual space (temporal retina, right column) is passed to the right hemisphere. Also note that a weakened, residual normal pathway still projects a portion of the left side of visual space (temporal retina, right column) to the left hemisphere. Bottom row: Eccentricity gradient response for left and right V1. Colors represent locations in visual space denoted by the legend at the top of the figure. Note that the left side of visual space (nasal retina, left column) is represented in right V1, as in the normal subject in (A). However, unlike the normal subject in (A), the majority of the right side of visual space (temporal retina, right column) is represented in right V1. Some of the right visual field is still represented in left V1, but not at the scale seen in the normal subject in (A).

ample of how intra-cortical self-organization during development allows abnormal representations to still subserve normal visual perception.

3.2.2. Achiasma

Albinism provided an example of how partial misrouting of the temporal retinal fibers can be successfully integrated into cortical topography as a mirror-symmetric map superimposed on the normal contralateral map. But what happens with a complete misrouting of the temporal retinal fibers? Is there a limit to the extent of such integration? Another relatively recently discovered congenital disorder called achiasma allows us to investigate these questions [118, 119].

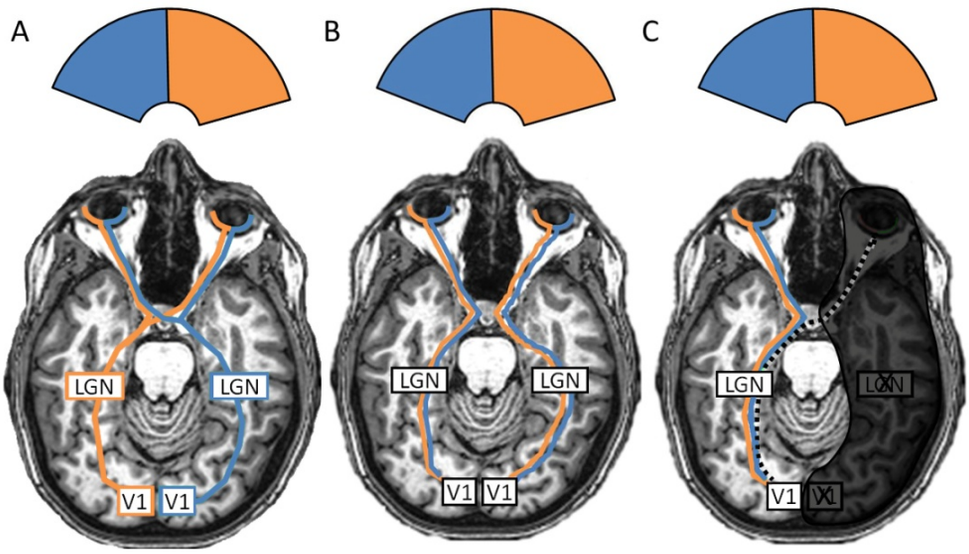

Figure 5. Visual Field Projections in Normal, Achiasmatic, and Missing Hemisphere Subjects. In all panels, blue represents the left half of visual space and tan represents the right side (top panel). (A) Normal subject. An image falling on the retinae is separated into nasal and temporal components in each eye. The part of the image within the left hemifield (blue) falls on the nasal retina in the left eye and the temporal retina in the right eye. The information from these two sections of each retina representing the left hemifield is transmitted through the optic nerve to the optic chiasm. To keep the correct hemifield information together for collective cortical processing, the axons from the nasal retina of the left eye cross over to the right optic tract at the optic chiasm, while the axons from the temporal retina of the right eye remain on the right side. Together, these sets of fibers carrying left hemifield image information then project first to the right lateral geniculate nucleus (LGN) of the thalamus and then through the optic radiations to V1 at the occipital pole of the right cortical hemisphere. Retinotopic organization is preserved along these pathways and then integrated into specific maps within visual cortex under the guidance of molecular cues and patterns of coordinated activity. The same pathways operate in reverse for the right hemifield (tan). Note that this results in one complete representation of visual space distributed across both hemispheres. (B) Achiasmatic subject. Because the fibers from the temporal retinae failed to properly cross at the expected region of the optic chiasm, information from each eye is passed only to the ipsilateral hemisphere. Thus, information from the left eye remains in the left hemisphere and information from the right eye remains in the right hemisphere. Note that this forms two complete representations of the full field of visual space, one for each eye, in each hemisphere. (C) Missing hemisphere subject. The development of the right hemisphere terminated in utero; therefore information from the left eye cannot possibly be passed to the right hemisphere. Instead, like achiasmatic subjects, the information remains in the ipsilateral hemisphere. Note that this means the entire visual field must be represented in the left hemisphere, resulting in one complete representation of visual space. The dotted black and white line represents possible remnants of connections to an undeveloped right eye.

Normally, molecular cues guide the axons of the retinal ganglion cells to either cross (temporal retinal fibers) to form the optic chiasm or to remain ipsilateral (nasal retinal fibers) (Figs. 4A, 5A). In individuals with achiasma, this crossing fails, with axons across each entire retina projecting through the ipsilateral thalamus to the ipsilateral cortical hemisphere (Fig. 5B) [118, 119]. The behavioral effects of this disorder can include deficits related to ocular instability (e.g., nystagmus, problems with stereopsis) [120 122].

Functional MRI was first used to investigate the topographical changes in achiasma by Victor et al. [120]. This study used a full field visual stimulus to show that stimulation of each eye produced functional activity within only the ipsilateral hemisphere. In addition, they found that the stimulation of each hemisphere produced overlapping activity within primary visual cortex. Their subjects had few visual deficits, other than problems related to ocular instability. These findings suggest successful integration of the misrouted visual pathways into the cortical topography. However, the pattern of cortical integration could not be determined from these methods.

With the development of higher resolution fMRI methods like TWR [34, 74] and pRF modeling [78], researchers have since been able to investigate more details about the topographical integration as well as changes in receptive field properties of regions within V1. A very recent study by Hoffman et al. [122] used both TWR and pRF to reveal that the congenital changes in achiasma drive developmental reorganization much like that seen in albinism. The complete misrouting of temporal retinal fibers was able to be successfully integrated as an overlapping, functional map of the ipsilateral visual field on top of that of the contralateral field (Fig. 5B). Further, the pRF measurements gave the first glimpse into human receptive field changes in these congenital disorders of visual pathway misrouting. Their results demonstrate pRFs that represent bilateral regions of the visual field in both striate and extrastriate VFMs along the medial occipital lobe.

Hoffman et al. [122] further used diffusion tensor imaging (DTI) to measure the general topography of the geniculostriate and occipital callosal connections in their achiasmatic subjects. Previous studies in achiasmatic dogs showed that the misrouted fibers formed retinotopic maps of opposing hemifields in adjacent layers of the LGN of the thalamus, suggesting no regorganization of geniculostriate pathways. The DTI measurements in human confirmed both that there were no significant changes in the input tracts to visual cortex as well as grossly normal topography in the inter-hemispheric callosal connections between the VFMs along the calcarine sulci. Together with the fMRI topographical and receptive field measurements, these findings by Hoffman et al. [122] suggest that the majority of the developmental reorganization in achiasma occurs in the intra-cortical local wiring within visual cortex.

3.3. How does the visual cortex reorganize following a massive cortical lesion in utero?

3.3.1. Missing hemisphere

In our last section, a dramatic recent example of a cortical lesion in utero allows us to examine the effects of a massive structural change to cortex on the development of cortical visual field representations. Muckli et al. [123] used TWR to study VFMs in a girl whose right cerebral

hemisphere was completely absent at birth (Fig. 5C). She has only a rudimentary right eye and right optic nerve, but no right optic tract. Despite this extensive cortical loss and absent right eye, this subject has mostly normal visual function in both hemifields, with a mild left hemiplegia. Her spared bilateral visual functions suggest an enormous degree of developmental cortical reorganization [124].

In this very unusual case, the right hemisphere failed to develop around the seventh week of gestation due to an in utero lesion. Therefore, no crossing of temporal retinal fibers to the contralateral LGN and cerebral hemisphere was possible. Instead, the axons from the left retina carrying information from the entire visual scene (both hemifields) could only project to the occipital lobe of the left hemisphere (Fig. 5C).

In this situation, what happens with the integration of the retinal fibers from the single eye? As with the development of the visual pathways in congenital disorders with grossly intact cortical structures, four primary possibilities exist. The first could be termed 'normal' development, in which the contralateral visual field develops as usual and no ipsilateral representation is created, leading to a full left hemianopsia. The second is the opposite of the first, such that only the ipsilateral field is represented, leading to total right hemianopsia following suppression of the normal contralateral representation. The third is that contiguous VFMs, representing both hemifields, develop either as complete maps or in patches in place of contralateral hemifields. Finally, superimposed or interdigitated representations of the contralateral and ipsilateral hemifields may develop, as seen in albinism and achiasma. In addition, it is possible that more than one of these organizational structures could exist concurrently among VFMs, as seen in some non-primate albino mammals.

Interestingly, the TWR measurements by Muckli et al. [123] demonstrate such a concurrent existence of more than one organizational pattern in her intact left hemisphere. In V1, contiguous representations of both the contra- and ipsilateral visual fields were superimposed within the calcarine sulcus. However, discrete islands of ipsilateral quarterfield representations were also measured along the vertical meridian of V2 and V3, with a distortion of the contralateral visual field representations.

Why in this case do we see full field maps in addition to the superposition found in albinism and achiasma? Perhaps reorganization at an earlier stage of the visual pathways has occurred here. Muckli et al. [123] examined the organization of the visual field representations in the remaining left LGN. Unlike the reorganization seen in albinism [114] and achiasma [122] in which the contra- and ipsilateral representations remained segregated in the LGN, the measurements in this subject appeared to be fully overlapping, suggesting a greater degree of reorganization at this stage of visual processing. Similar LGN reorganization was measured in some albino cats and ferrets, which also had at least sections of contiguous full field visual field representations in their primary visual cortex [107-110].

The organization of the visual field representations is reflected in the extent of her preserved visual function. First, the fact that she has intact vision in the ipsilateral, right visual field demonstrates that the novel ipsilateral visual field representations are functionally relevant.

Second, visual perimetry mapping showed that both the right and left visual fields were centrally intact, but that both were somewhat restricted. Interestingly, the insertion of the ipsilateral islands into the contralateral representations resulted in both distortions of the cortical contralateral representations as well as concurrent distortions of her functional contralateral visual field. This restriction was more prominent in the upper visual field of both fields, in accord with the greater distortion of the contralateral visual field representation on the ventral cortical surface. The different patterns of self-organization in these VFMs in this unique case demonstrate a surprisingly flexible developmental restructuring in response to massive cortical loss.

4. Conclusion

This chapter has examined fMRI measurements of naturally-occurring cortical reorganization due to congenital abnormalities in the developing human visual system. These examples of retinal and genetic changes and cortical loss highlight the roles of plasticity and stability in the developing visual system. In these congenital conditions, the abnormally represented visual information has become available for grossly normal visual perception, despite limited compensatory alterations in the relatively stable geniculostriate projections. Together, these studies suggest that instead of large-scale reorganizations of the afferent visual pathways, relatively less drastic intra-cortical mechanisms underlie such developmental plasticity.

The next essential expansion of these findings is to apply our understanding of developmental plasticity to the controversial field of plasticity in adult sensory systems. Several aspects of cortical organization are thought to remain plastic into adulthood, allowing cortical sensorimotor maps to be modified continuously by experience. This dynamic nature of cortical circuitry is important for learning, as well as for repair following nervous system injury. Studies of the extent of cortical reorganization in adult primate visual cortex in response to changes in sensory input have produced quite disparate results, however (e.g., [1, 2, 125-138]). The ability to control cortical reorganization in the adult either by harnessing existing adult mechanisms for plasticity or by reactivating mechanisms of developmental plasticity would be a tremendous advancement in the treatment of cortical damage and neurodegenerative disease. The understanding of the balance of plasticity and stability in the human visual system arising from the examination of such congenital visual disorders as described here will be a key element of our progress towards this goal.

Acknowledgment

This work was supported by University of California, Irvine, startup funds to A.A.B.

Author details

Alyssa A. Brewer and Brian Barton

Center for Cognitive Neuroscience and Department of Cognitive Sciences, University of California, Irvine, USA

References

[1] J. C. Horton and D. R. Hocking, "Timing of the critical period for plasticity of ocular dominance columns in macaque striate cortex," J Neurosci, vol. 17, pp. 3684-709, May 15 1997.

[2] J. C. Horton and D. R. Hocking, "Effect of early monocular enucleation upon ocular dominance columns and cytochrome oxidase activity in monkey and human visual cortex," Vis Neurosci, vol. 15, pp. 289-303, Mar-Apr 1998.

[3] D. D. O'Leary, N. L. Ruff, and R. H. Dyck, "Development, critical period plasticity, and adult reorganizations of mammalian somatosensory systems," Curr Opin Neurobiol, vol. 4, pp. 535-44, Aug 1994.

[4] T. K. Hensch, "Critical period plasticity in local cortical circuits," Nat Rev Neurosci, vol. 6, pp. 877-88, Nov 2005.

[5] B. A. Wandell and S. M. Smirnakis, "Plasticity and stability of visual field maps in adult primary visual cortex," Nat Rev Neurosci, vol. 10, pp. 873-84, Dec 2009.

[6] S. M. Smirnakis, A. A. Brewer, M. C. Schmid, A. S. Tolias, A. Schuz, M. Augath, W. Inhoffen, B. A. Wandell, and N. K. Logothetis, "Lack of long-term cortical reorganization after macaque retinal lesions," Nature, vol. 435, pp. 300-7, May 19 2005.

[7] D. V. Buonomano and M. M. Merzenich, "Cortical plasticity: from synapses to maps," Annu Rev Neurosci, vol. 21, pp. 149-86, 1998.

[8] M. M. Merzenich, R. J. Nelson, M. P. Stryker, M. S. Cynader, A. Schoppmann, and J. M. Zook, "Somatosensory cortical map changes following digit amputation in adult monkeys," J Comp Neurol, vol. 224, pp. 591-605, Apr 20 1984.

[9] J. H. Kaas, M. M. Merzenich, and H. P. Killackey, "The reorganization of somatosensory cortex following peripheral nerve damage in adult and developing mammals," Annu Rev Neurosci, vol. 6, pp. 325-56, 1983.

[10] L. G. Cohen, P. Celnik, A. Pascual-Leone, B. Corwell, L. Falz, J. Dambrosia, M. Honda, N. Sadato, C. Gerloff, M. D. Catala, and M. Hallett, "Functional relevance of cross-modal plasticity in blind humans," Nature, vol. 389, pp. 180-3, Sep 11 1997.

[11] K. Fox and R. O. Wong, "A comparison of experience-dependent plasticity in the visual and somatosensory systems," Neuron, vol. 48, pp. 465-77, Nov 3 2005.

[12] C. D. Gilbert, W. Li, and V. Piech, "Perceptual learning and adult cortical plasticity," J Physiol, vol. 587, pp. 2743-51, Jun 15 2009.

[13] C. J. Shatz, "Emergence of order in visual system development," Proc Natl Acad Sci U S A, vol. 93, pp. 602-8, Jan 23 1996.

[14] D. H. Hubel, T. N. Wiesel, and S. LeVay, "Plasticity of ocular dominance columns in monkey striate cortex," Philos Trans R Soc Lond B Biol Sci, vol. 278, pp. 377-409, Apr 26 1977.

[15] B. Chapman, I. Godecke, and T. Bonhoeffer, "Development of orientation preference in the mammalian visual cortex," J Neurobiol, vol. 41, pp. 18-24, Oct 1999.

[16] M. Weliky and L. C. Katz, "Correlational structure of spontaneous neuronal activity in the developing lateral geniculate nucleus in vivo [see comments]," Science, vol. 285, pp. 599-604, 1999.

[17] L. C. Katz and C. J. Shatz, "Synaptic activity and the construction of cortical circuits," Science, vol. 274, pp. 1133-8, Nov 15 1996.

[18] C. J. Shatz and M. P. Stryker, "Ocular dominance in layer IV of the cat's visual cortex and the effects of monocular deprivation," J Physiol, vol. 281, pp. 267-83, Aug 1978.

[19] D. C. Van Essen, "Behind the optic nerve: an inside view of the primate visual system," Trans Am Ophthalmol Soc, vol. 93, pp. 123-33, 1995.

[20] J. C. Horton and D. R. Hocking, "An adult-like pattern of ocular dominance columns in striate cortex of newborn monkeys prior to visual experience.," Journal of Neuroscience, vol. 16, pp. 1791-1807, 1996.

[21] D. H. Hubel and T. N. Wiesel, "Receptive Fields of Cells in Striate Cortex of Very Young, Visually Inexperienced Kittens," J Neurophysiol, vol. 26, pp. 994-1002, Nov 1963.

[22] D. H. Hubel, T. N. Wiesel, and S. LeVay, "Functional architecture of area 17 in normal and monocularly deprived macaque monkeys," Cold Spring Harb Symp Quant Biol, vol. 40, pp. 581-9, 1976.

[23] T. N. Wiesel and D. H. Hubel, "Ordered arrangement of orientation columns in monkeys lacking visual experience," J Comp Neurol, vol. 158, pp. 307-18, Dec 1 1974.

[24] S. LeVay, M. P. Stryker, and C. J. Shatz, "Ocular dominance columns and their development in layer IV of the cat's visual cortex: a quantitative study.," Journal of Comparative Neurology, vol. 179, pp. 223-244, 1978.

[25] P. Rakic and M. S. Lidow, "Distribution and density of mnoamine receptor s in the primate visual cortex devoid of retinal input from early embryonic stagesemut f," J. Neuroscience, vol. 15, pp. 256-2574, 1995.

[26] D. Stellwagen, C. J. Shatz, and M. B. Feller, "Dynamics of retinal waves are controlled by cyclic AMP," Neuron, vol. 24, pp. 673-85, Nov 1999.

[27] M. P. Stryker and W. A. Harris, "Binocular impulse blockade prevents the formation of ocular dominance columns in cat visual cortex," J Neurosci, vol. 6, pp. 2117-33, Aug 1986.

[28] C. Zetterstrom, A. Lundvall, and M. Kugelberg, "Cataracts in children," J Cataract Refract Surg, vol. 31, pp. 824-40, Apr 2005.

[29] S. Awaya and S. Miyake, "Form vision deprivation amblyopia: further observations," Graefes Arch Clin Exp Ophthalmol, vol. 226, pp. 132-6, 1988.

[30] X. Li, S. O. Dumoulin, B. Mansouri, and R. F. Hess, "The fidelity of the cortical retinotopic map in human amblyopia," Eur J Neurosci, vol. 25, pp. 1265-77, Mar 2007.

[31] X. Li, S. O. Dumoulin, B. Mansouri, and R. F. Hess, "Cortical deficits in human amblyopia: their regional distribution and their relationship to the contrast detection deficit," Invest Ophthalmol Vis Sci, vol. 48, pp. 1575-91, Apr 2007.

[32] A. A. Brewer and B. Barton, "Visual field map organization in human visual cortex," in Visual Cortex - Current Status and Perspectives, S. Molotchnikoff and J. Rouat, Eds., ed: InTech, 2012, pp. 30-60.

[33] B. A. Wandell, A. A. Brewer, and R. F. Dougherty, "Visual field map clusters in human cortex," Philos Trans R Soc Lond B Biol Sci, vol. 360, pp. 693-707, Apr 29 2005.

[34] B. A. Wandell, S. O. Dumoulin, and A. A. Brewer, "Visual field maps in human cortex," Neuron, vol. 56, pp. 366-83, Oct 25 2007.

[35] D. C. Van Essen, "Organization of Visual Areas in Macaque and Human Cerebral Cortex," in The Visual Neurosciences, L. M. Chalupa and J. S. Werner, Eds., ed Boston: Bradford Books, 2003.

[36] J. H. Kaas, "Topographic Maps are Fundamental to Sensory Processing," Brain Research Bulletin, vol. 44, pp. 107–112, 1997.

[37] S. Zeki, "Improbable areas in the visual brain," Trends Neurosci, vol. 26, pp. 23-6, Jan 2003.

[38] B. A. Wandell and J. Winawer, "Imaging retinotopic maps in the human brain," Vision Res, Aug 6 2010.

[39] N. K. Logothetis and B. A. Wandell, "Interpreting the BOLD signal," Annu Rev Physiol, vol. 66, pp. 735-69, 2004.

[40] S. Ogawa, T. M. Lee, A. R. Kay, and D. W. Tank, "Brain magnetic resonance imaging with contrast dependent on blood oxygenation," Proc Natl Acad Sci U S A, vol. 87, pp. 9868-72, Dec 1990.

[41] D. J. Heeger and D. Ress, "What does fMRI tell us about neuronal activity?," Nat Rev Neurosci, vol. 3, pp. 142-51, Feb 2002.

[42] P. A. Bandettini, E. C. Wong, R. S. Hinks, R. S. Tikofsky, and J. S. Hyde, "Time course EPI of human brain function during task activation," Magn Reson Med, vol. 25, pp. 390-7, Jun 1992.

[43] A. K. Liu, J. W. Belliveau, and A. M. Dale, "Spatiotemporal imaging of human brain activity using functional MRI constrained magnetoencephalography data: Monte Carlo simulations," Proc Natl Acad Sci U S A, vol. 95, pp. 8945-50, Jul 21 1998.

[44] M. B. Hoffmann, J. Stadler, M. Kanowski, and O. Speck, "Retinotopic mapping of the human visual cortex at a magnetic field strength of 7T," Clin Neurophysiol, vol. 120, pp. 108-16, Jan 2009.

[45] J. D. Swisher, J. C. Gatenby, J. C. Gore, B. A. Wolfe, C. H. Moon, S. G. Kim, and F. Tong, "Multiscale pattern analysis of orientation-selective activity in the primary visual cortex," J Neurosci, vol. 30, pp. 325-30, Jan 6 2010.

[46] C. Triantafyllou, R. D. Hoge, G. Krueger, C. J. Wiggins, A. Potthast, G. C. Wiggins, and L. L. Wald, "Comparison of physiological noise at 1.5 T, 3 T and 7 T and optimization of fMRI acquisition parameters," Neuroimage, vol. 26, pp. 243-50, May 15 2005.

[47] E. Disbrow, T. P. Roberts, D. Slutsky, and L. Krubitzer, "The use of fMRI for determining the topographic organization of cortical fields in human and nonhuman primates," Brain Res, vol. 829, pp. 167-73, May 22 1999.

[48] N. K. Logothetis, "What we can do and what we cannot do with fMRI," Nature, vol. 453, pp. 869-78, Jun 12 2008.

[49] Y. Ejima, S. Takahashi, H. Yamamoto, M. Fukunaga, C. Tanaka, T. Ebisu, and M. Umeda, "Interindividual and interspecies variations of the extrastriate visual cortex," Neuroreport, vol. 14, pp. 1579-83, Aug 26 2003.

[50] N. K. Chen and A. M. Wyrwicz, "Correction for EPI distortions using multi-echo gradient-echo imaging," Magn Reson Med, vol. 41, pp. 1206-13, Jun 1999.

[51] M. Lauritzen, "Relationship of spikes, synaptic activity, and local changes of cerebral blood flow," J Cereb Blood Flow Metab, vol. 21, pp. 1367-83, Dec 2001.

[52] A. Seiyama, J. Seki, H. C. Tanabe, I. Sase, A. Takatsuki, S. Miyauchi, H. Eda, S. Hayashi, T. Imaruoka, T. Iwakura, and T. Yanagida, "Circulatory basis of fMRI signals: relationship between changes in the hemodynamic parameters and BOLD signal intensity," Neuroimage, vol. 21, pp. 1204-14, Apr 2004.

[53] J. Winawer, H. Horiguchi, R. A. Sayres, K. Amano, and B. A. Wandell, "Mapping hV4 and ventral occipital cortex: the venous eclipse," J Vis, vol. 10, p. 1, 2010.

[54] A. A. Brewer, J. Liu, A. R. Wade, and B. A. Wandell, "Visual field maps and stimulus selectivity in human ventral occipital cortex," Nat Neurosci, vol. 8, pp. 1102-9, Aug 2005.

[55] K. A. Hansen, K. N. Kay, and J. L. Gallant, "Topographic organization in and near human visual area V4," J Neurosci, vol. 27, pp. 11896-911, Oct 31 2007.

[56] A. R. Wade, A. A. Brewer, J. W. Rieger, and B. A. Wandell, "Functional measurements of human ventral occipital cortex: retinotopy and colour," Philos Trans R Soc Lond B Biol Sci, vol. 357, pp. 963-73, Aug 29 2002.

[57] J. Larsson and D. J. Heeger, "Two retinotopic visual areas in human lateral occipital cortex," J Neurosci, vol. 26, pp. 13128-42, Dec 20 2006.

[58] R. B. Tootell and N. Hadjikhani, "Where is 'dorsal V4' in human visual cortex? Retinotopic, topographic and functional evidence," Cereb Cortex, vol. 11, pp. 298-311, Apr 2001.

[59] N. Hadjikhani, A. K. Liu, A. M. Dale, P. Cavanagh, and R. B. Tootell, "Retinotopy and color sensitivity in human visual cortical area V8," Nat Neurosci, vol. 1, pp. 235-41, Jul 1998.

[60] B. A. Wandell, S. Chial, and B. Backus, "Visualization and Measurement of the Cortical Surface," J. of Cognitive Neuroscience, vol. 12, pp. 739-52, 2000.

[61] P. C. Teo, G. Sapiro, and B. A. Wandell, "Creating connected representations of cortical gray matter for functional MRI visualization," IEEE Trans Med Imaging, vol. 16, pp. 852-63, Dec 1997.

[62] D. C. Van Essen, J. W. Lewis, H. A. Drury, N. Hadjikhani, R. B. Tootell, M. Bakircioglu, and M. I. Miller, "Mapping visual cortex in monkeys and humans using surface-based atlases," Vision Res, vol. 41, pp. 1359-78, 2001.

[63] A. M. Dale, B. Fischl, and M. I. Sereno, "Cortical surface-based analysis. I. Segmentation and surface reconstruction," Neuroimage, vol. 9, pp. 179-94, Feb 1999.

[64] H. Kolster, R. Peeters, and G. A. Orban, "The retinotopic organization of the human middle temporal area MT/V5 and its cortical neighbors," J Neurosci, vol. 30, pp. 9801-20, Jul 21 2010.

[65] X. Yue, B. S. Cassidy, K. J. Devaney, D. J. Holt, and R. B. Tootell, "Lower-level stimulus features strongly influence responses in the fusiform face area," Cereb Cortex, vol. 21, pp. 35-47, Jan 2011.

[66] T. Liu, F. Pestilli, and M. Carrasco, "Transient attention enhances perceptual performance and FMRI response in human visual cortex," Neuron, vol. 45, pp. 469-77, Feb 3 2005.

[67] J. S. Peper, R. M. Brouwer, D. I. Boomsma, R. S. Kahn, and H. E. Hulshoff Pol, "Genetic influences on human brain structure: a review of brain imaging studies in twins," Hum Brain Mapp, vol. 28, pp. 464-73, Jun 2007.

[68] W. F. Baare, H. E. Hulshoff Pol, D. I. Boomsma, D. Posthuma, E. J. de Geus, H. G. Schnack, N. E. van Haren, C. J. van Oel, and R. S. Kahn, "Quantitative genetic modeling of variation in human brain morphology," Cereb Cortex, vol. 11, pp. 816-24, Sep 2001.

[69] R. F. Dougherty, V. M. Koch, A. A. Brewer, B. Fischer, J. Modersitzki, and B. A. Wandell, "Visual field representations and locations of visual areas V1/2/3 in human visual cortex," J Vis, vol. 3, pp. 586-98, 2003.

[70] M. P. Bryden, H. Hecaen, and M. DeAgostini, "Patterns of cerebral organization," Brain Lang, vol. 20, pp. 249-62, Nov 1983.

[71] R. A. Harshman, E. Hampson, and S. A. Berenbaum, "Individual differences in cognitive abilities and brain organization, Part I: Sex and handedness differences in ability," Can J Psychol, vol. 37, pp. 144-92, Mar 1983.

[72] J. H. Kaas, "The evolution of the complex sensory and motor systems of the human brain," Brain Res Bull, vol. 75, pp. 384-90, Mar 18 2008.

[73] S. A. Engel, G. H. Glover, and B. A. Wandell, "Retinotopic organization in human visual cortex and the spatial precision of functional MRI," Cereb Cortex, vol. 7, pp. 181-92, Mar 1997.

[74] S. A. Engel, D. E. Rumelhart, B. A. Wandell, A. T. Lee, G. H. Glover, E. J. Chichilnisky, and M. N. Shadlen, "fMRI of human visual cortex," Nature, vol. 369, p. 525, Jun 16 1994.

[75] M. I. Sereno, A. M. Dale, J. B. Reppas, K. K. Kwong, J. W. Belliveau, T. J. Brady, B. R. Rosen, and R. B. Tootell, "Borders of multiple visual areas in humans revealed by functional magnetic resonance imaging," Science, vol. 268, pp. 889-93, May 12 1995.

[76] E. A. DeYoe, G. J. Carman, P. Bandettini, S. Glickman, J. Wieser, R. Cox, D. Miller, and J. Neitz, "Mapping striate and extrastriate visual areas in human cerebral cortex," Proc. Natl. Acad. Sci. (USA), vol. 93, pp. 2382-2386, 1996.

[77] S. A. Engel, "The development and use of phase-encoded functional MRI designs," Neuroimage, vol. 62, pp. 1195 - 200, Aug 15 2012.

[78] S. O. Dumoulin and B. A. Wandell, "Population receptive field estimates in human visual cortex," Neuroimage, vol. 39, pp. 647-60, Jan 15 2008.

[79] A. T. Smith, K. D. Singh, A. L. Williams, and M. W. Greenlee, "Estimating receptive field size from fMRI data in human striate and extrastriate visual cortex," Cereb Cortex, vol. 11, pp. 1182-90, Dec 2001.

[80] B. A. Wandell and J. Winawer, "Imaging retinotopic maps in the human brain," Vision Res, vol. 51, pp. 718-37, Apr 13 2011.

[81] K. Amano, B. A. Wandell, and S. O. Dumoulin, "Visual field maps, population receptive field sizes, and visual field coverage in the human MT+ complex," Journal of Neurophysiology, vol. 102, pp. 2704-18, Nov 2009.

[82] J. D. Victor, K. Purpura, E. Katz, and B. Mao, "Population encoding of spatial frequency, orientation, and color in macaque V1," J Neurophysiol, vol. 72, pp. 2151-66, Nov 1994.

[83] R. B. Tootell, J. D. Mendola, N. K. Hadjikhani, P. J. Ledden, A. K. Liu, J. B. Reppas, M. I. Sereno, and A. M. Dale, "Functional analysis of V3A and related areas in human visual cortex," J Neurosci, vol. 17, pp. 7060-78, Sep 15 1997.

[84] B. M. Harvey and S. O. Dumoulin, "The relationship between cortical magnification factor and population receptive field size in human visual cortex: constancies in cortical architecture," J Neurosci, vol. 31, pp. 13604-12, Sep 21 2011.

[85] M. I. Sereno, H. H. Yu, and E. K. Vogel, "Mapping Retinotopy in Higher Level Extrastriate Visual Areas in Humans," in Society for Neuroscience, San Diego, 2001.

[86] M. I. Sereno, S. Pitzalis, and A. Martinez, "Mapping of contralateral space in retinotopic coordinates by a parietal cortical area in humans," Science, vol. 294, pp. 1350-4, Nov 9 2001.

[87] W. Zuiderbaan, B. M. Harvey, and S. O. Dumoulin, "Modeling center-surround configurations in population receptive fields using fMRI," J Vis, vol. 12, p. 10, 2012.

[88] H. J. Neville and D. Bavelier, "Variability of developmental plasticity," in Mechanisms of Cognitive Develoment: Behavioral and Neural Perspectives, J. L. McClelland and R. S. Siegler, Eds., ed New Jersey: Lawrence Erlbaum Associates, Inc., 2001.

[89] M. M. Merzenich and K. Sameshima, "Cortical plasticity and memory," Curr Opin Neurobiol, vol. 3, pp. 187-96, Apr 1993.

[90] P. Sinha and M. Meng, "Superimposed hemifields in primary visual cortex of achiasmic individuals," Neuron, vol. 75, pp. 353-5, Aug 9 2012.

[91] C. A. Curcio, K. R. Sloan, R. E. Kalina, and A. E. Hendrickson, "Human photoreceptor topography," J Comp Neurol, vol. 292, pp. 497-523, Feb 22 1990.

[92] C. A. Curcio, K. R. S. Jr., O. Pakcer, A. E. Hendrickson, and R. E. Kalina, "Distribution of cones in human and monkey retina: individual variaibility and radial asymmetry," in Science, 1987, pp. 579-581.

[93] K. R. Duffy and D. H. Hubel, "Receptive field properties of neurons in the primary visual cortex under photopic and scotopic lighting conditions," Vision Res, vol. 47, pp. 2569-74, Sep 2007.

[94] J. C. Horton and W. F. Hoyt, "The representation of the visual field in human striate cortex. A revision of the classic Holmes map," Arch Ophthalmol, vol. 109, pp. 816-24, Jun 1991.

[95] H. A. Baseler, A. A. Brewer, L. T. Sharpe, A. B. Morland, H. Jagle, and B. A. Wandell, "Reorganization of human cortical maps caused by inherited photoreceptor abnormalities," Nat Neurosci, vol. 5, pp. 364-70, Apr 2002.

[96] N. Hadjikhani and R. B. Tootell, "Projection of rods and cones within human visual cortex," Hum Brain Mapp, vol. 9, pp. 55-63, 2000.

[97] D. H. Hubel, "Vision in dim light," Nature, vol. 388, pp. 32-3, Jul 3 1997.

[98] D. H. Hubel, P. D. Howe, A. M. Duffy, and A. Hernandez, "Scotopic foveal afterimages," Perception, vol. 38, pp. 313-6, 2009.

[99] S. Kohl, B. Baumann, M. Broghammer, H. Jagle, P. Sieving, U. Kellner, R. Spegal, M. Anastasi, E. Zrenner, L. T. Sharpe, and B. Wissinger, "Mutations in the CNGB3 gene encoding the beta-subunit of the cone photoreceptor cGMP-gated channel are responsible for achromatopsia (ACHM3) linked to chromosome 8q21," Hum Mol Genet, vol. 9, pp. 2107-16, Sep 1 2000.

[100] S. Kohl, T. Marx, I. Giddings, H. Jagle, S. G. Jacobson, E. Apfelstedt-Sylla, E. Zrenner, L. T. Sharpe, and B. Wissinger, "Total colourblindness is caused by mutations in the gene encoding the alpha-subunit of the cone photoreceptor cGMP-gated cation channel," Nat Genet, vol. 19, pp. 257-9, Jul 1998.

[101] M. Glickstein and G. G. Heath, "Receptors in the monochromat eye," Vision Res, vol. 15, pp. 633-6, Jun 1975.

[102] J. L. Rees, "Genetics of hair and skin color," Annu Rev Genet, vol. 37, pp. 67-90, 2003.

[103] P. Hedera, S. Lai, E. M. Haacke, A. J. Lerner, A. L. Hopkins, J. S. Lewin, and R. P. Friedland, "Abnormal connectivity of the visual pathways in human albinos demonstrated by susceptibility-sensitized MRI," Neurology, vol. 44, pp. 1921-6, Oct 1994.

[104] A. B. Morland, M. B. Hoffmann, M. Neveu, and G. E. Holder, "Abnormal visual projection in a human albino studied with functional magnetic resonance imaging and visual evoked potentials," J Neurol Neurosurg Psychiatry, vol. 72, pp. 523-6, Apr 2002.

[105] R. W. Guillery, "Neural abnormalities of albinos," Trends in Neurosciences, vol. 9, pp. 364-367, 1986.

[106] A. B. Morland, H. A. Baseler, M. B. Hoffmann, L. T. Sharpe, and B. A. Wandell, "Abnormal retinotopic representations in human visual cortex revealed by fMRI," Acta Psychol (Amst), vol. 107, pp. 229-47, Apr 2001.

[107] R. W. Guillery, V. A. Casagrande, and M. D. Oberdorfer, "Congenitally abnormal vision in Siamese cats," Nature, vol. 252, pp. 195-9, Nov 15 1974.

[108] D. H. Hubel and T. N. Wiesel, "Aberrant visual projections in the Siamese cat," J Physiol, vol. 218, pp. 33-62, Oct 1971.

[109] K. Huang and R. W. Guillery, "A demonstration of two distinct geniculocortical projection patterns in albino ferrets," Brain Res, vol. 352, pp. 213-20, Jun 1985.

[110] J. H. Kaas and R. W. Guillery, "The transfer of abnormal visual field representations from the dorsal lateral geniculate nucleus to the visual cortex in Siamese cats," Brain Res, vol. 59, pp. 61-95, Sep 14 1973.

[111] E. I. Elekessy, J. E. Campion, and G. H. Henry, "Differences between the visual fields of Siamese and common cats," Vision Res, vol. 13, pp. 2533-43, Dec 1973.

[112] M. L. Cooper and G. G. Blasdel, "Regional variation in the representation of the visual field in the visual cortex of the Siamese cat," J Comp Neurol, vol. 193, pp. 237-53, Sep 1 1980.

[113] R. W. Guillery, T. L. Hickey, J. H. Kaas, D. J. Felleman, E. J. Debruyn, and D. L. Sparks, "Abnormal central visual pathways in the brain of an albino green monkey (Cercopithecus aethiops)," J Comp Neurol, vol. 226, pp. 165-83, Jun 20 1984.

[114] M. B. Hoffmann, D. J. Tolhurst, A. T. Moore, and A. B. Morland, "Organization of the visual cortex in human albinism," J Neurosci, vol. 23, pp. 8921-30, Oct 1 2003.

[115] M. B. Hoffmann, P. S. Seufert, and L. C. Schmidtborn, "Perceptual relevance of abnormal visual field representations: static visual field perimetry in human albinism," Br J Ophthalmol, vol. 91, pp. 509-13, Apr 2007.

[116] M. B. Hoffmann, B. Lorenz, A. B. Morland, and L. C. Schmidtborn, "Misrouting of the optic nerves in albinism: estimation of the extent with visual evoked potentials," Invest Ophthalmol Vis Sci, vol. 46, pp. 3892-8, Oct 2005.

[117] J. Klemen, M. B. Hoffmann, and C. D. Chambers, "Cortical plasticity in the face of congenitally altered input into V1," Cortex, Mar 23 2012.

[118] P. Apkarian, L. Bour, and P. G. Barth, "A unique achiasmatic anomaly detected in non-albinos with misrouted retinal fugal projections," Eur J Neurosci, vol. 6, pp. 501-7, Mar 1 1994.

[119] P. Apkarian, L. J. Bour, P. G. Barth, L. Wenniger-Prick, and B. Verbeeten, Jr., "Non-decussating retinal-fugal fibre syndrome. An inborn achiasmatic malformation associated with visuotopic misrouting, visual evoked potential ipsilateral asymmetry and nystagmus," Brain, vol. 118 (Pt 5), pp. 1195-216, Oct 1995.

[120] J. D. Victor, P. Apkarian, J. Hirsch, M. M. Conte, M. Packard, N. R. Relkin, K. H. Kim, and R. M. Shapley, "Visual function and brain organization in non-decussating retinal-fugal fibre syndrome," Cereb Cortex, vol. 10, pp. 2-22, Jan 2000.

[121] S. Prakash, S. O. Dumoulin, N. Fischbein, B. A. Wandell, and Y. J. Liao, "Congenital achiasma and see-saw nystagmus in VACTERL syndrome," J Neuroophthalmol, vol. 30, pp. 45-8, Mar 2010.

[122] M. B. Hoffmann, F. R. Kaule, N. Levin, Y. Masuda, A. Kumar, I. Gottlob, H. Horiguchi, R. F. Dougherty, J. Stadler, B. Wolynski, O. Speck, M. Kanowski, Y. J. Liao, B. A. Wandell, and S. O. Dumoulin, "Plasticity and stability of the visual system in human achiasma," Neuron, vol. 75, pp. 393-401, Aug 9 2012.

[123] L. Muckli, M. J. Naumer, and W. Singer, "Bilateral visual field maps in a patient with only one hemisphere," Proc Natl Acad Sci U S A, vol. 106, pp. 13034-9, Aug 4 2009.

[124] A. A. Brewer, "Visual maps: To merge or not to merge," Curr Biol, vol. 19, pp. R945-7, Nov 3 2009.

[125] C. Darian-Smith and C. D. Gilbert, "Axonal sprouting accompanies functional reorganization in adult cat striate cortex.," Nature, vol. 368, pp. 737-740, 1994.

[126] G. C. DeAngelis, A. Anzai, I. Ohzawa, and R. D. Freeman, "Receptive field structure in the visual cortex: does selective stimulation induce plasticity?," Proc Natl Acad Sci U S A, vol. 92, pp. 9682-6, Oct 10 1995.

[127] J. C. Horton and D. R. Hocking, "Monocular core zones and binocular border strips in primate striate cortex revealed by the contrasting effects of enucleation, eyelid suture, and retinal laser lesions on cytochrome oxidase activity," J Neurosci, vol. 18, pp. 5433-55, Jul 15 1998.

[128] J. H. Kaas, "Plasticity of sensory and motor maps in adult mammals.," Annual Review of Neuroscience, vol. 14, pp. 137-167, 1991.

[129] C. I. Baker, E. Peli, N. Knouf, and N. G. Kanwisher, "Reorganization of visual processing in macular degeneration," J Neurosci, vol. 25, pp. 614-8, Jan 19 2005.

[130] C. D. Gilbert and T. N. Wiesel, "Receptive field dynamics in adult primary visual cortex," Nature, vol. 356, pp. 150-2, Mar 12 1992.

[131] Y. M. Chino, J. H. Kaas, E. L. Smith, 3rd, A. L. Langston, and H. Cheng, "Rapid reorganization of cortical maps in adult cats following restricted deafferentation in retina," Vision Res, vol. 32, pp. 789-96, May 1992.

[132] C. Darian-Smith and C. D. Gilbert, "Topographic reorganization in the striate cortex of the adult cat and monkey is cortically mediated," J Neurosci, vol. 15, pp. 1631-47, Mar 1995.

[133] A. Das and C. D. Gilbert, "Topography of contextual modulations mediated by short-range interactions in primary visual cortex," Nature, vol. 399, pp. 655-61, Jun 17 1999.

[134] A. Das and C. D. Gilbert, "Long-range horizontal connections and their role in cortical reorganization revealed by optical recording of cat primary visual cortex," Nature, vol. 375, pp. 780-4, Jun 29 1995.

[135] J. S. Sunness, T. Liu, and S. Yantis, "Retinotopic mapping of the visual cortex using functional magnetic resonance imaging in a patient with central scotomas from atrophic macular degeneration," Ophthalmology, vol. 111, pp. 1595-8, Aug 2004.

[136] J. H. Kaas, L. A. Krubitzer, Y. M. Chino, A. L. Langston, E. H. Polley, and N. Blair, "Reorganization of retinotopic cortical maps in adult mammals after lesions of the retina," Science, vol. 248, pp. 229-31, Apr 13 1990.

[137] H. A. Baseler, A. B. Morland, and B. A. Wandell, "Topographic organization of human visual areas in the absence of input from primary cortex," J Neurosci, vol. 19, pp. 2619-27, Apr 1 1999.

[138] C. D. Gilbert, "Adult cortical dynamics," Physiol Rev, vol. 78, pp. 467-85, Apr 1998.